ResearchGate

See discussions, stats, and author profiles for this publication at: https://www.researchgate.net/publication/274900736

Evolution of DNA Aptamers through in vitro Metastatic-cell-based SELEX for Metastatic Cancer Recognition and Imaging

ARTICLE *in* ANALYTICAL CHEMISTRY · APRIL 2015

Impact Factor: 5.64 · DOI: 10.1021/acs.analchem.5b00637 · Source: PubMed

CITATIONS
2

READS
41

10 AUTHORS, INCLUDING:

Zhi Zhu
China Medical University (ROC)
171 PUBLICATIONS **3,574** CITATIONS
SEE PROFILE

Hao Linlin
National University of Singapore
9 PUBLICATIONS **12** CITATIONS
SEE PROFILE

Chaoyong James Yang
Xiamen University
123 PUBLICATIONS **4,605** CITATIONS
SEE PROFILE

Available from: Chaoyong James Yang
Retrieved on: 31 January 2016

analytical chemistry

Article

pubs.acs.org/ac

Evolution of DNA Aptamers through in Vitro Metastatic-Cell-Based Systematic Evolution of Ligands by Exponential Enrichment for Metastatic Cancer Recognition and Imaging

Xilan Li,[†] Yuan An,[†] Jiang Jin,[‡] Zhi Zhu,[†] Linlin Hao,[§] Lu Liu,[†] Yongquan Shi,[‡] Daiming Fan,[‡] Tianhai Ji,[†] and Chaoyong James Yang*[,†]

[†]State Key Laboratory of Physical Chemistry of Solid Surfaces, The MOE Key Laboratory of Spectrochemical Analysis and Instrumentation, Collaborative Innovation Center of Chemistry for Energy Materials, Key Laboratory for Chemical Biology of Fujian Province, Department of Chemical Biology, College of Chemistry and Chemical Engineering, Affiliated Chenggong Hospital, Xiamen University, Xiamen 361005, People's Republic of China

[‡]State Key Laboratory of Cancer Biology and Xijing Hospital of Digestive Diseases, Xijing Hospital, Fourth Military Medical University, Xi'an 710032, Shaanxi Province, People's Republic of China

[§]State Key Laboratory of Urban Water Resource and Environment, School of Municipal and Environmental Engineering, Harbin Institute of Technology, Harbin 150090, People's Republic of China

Supporting Information

ABSTRACT: Metastasis, the capability of tumor cells to spread and grow at distant sites, is the primary factor in cancer mortality. Because metastasis in sentinel lymph nodes suggests the original spread of tumors from a primary site, the detection of lymph node involvement with cancer serves as an important prognostic and treatment parameter. Here we have developed a panel of DNA aptamers specifically binding to colon cancer cell SW620 derived from metastatic site lymph node, with high affinity after 14 rounds of selection by the cell-SELEX (systematic evolution of ligands by exponential enrichment) method. The binding affinities of selected aptamers were evaluated by flow cytometry. Aptamer XL-33 with the best binding affinity (0.7 nM) and its truncated sequence XL-33-1 with 45 nt showed excellent selectivity for recognizing target cell SW620. The binding entity of the selected aptamer has been preliminarily determined as a membrane protein on the cell surface. Tissue imaging results showed that XL-33-1 was highly specific to the metastatic tumor tissue or lymph node tissue with corresponding cancer metastasis and displayed an 81.7% detection rate against colon cancer tissue with metastasis in regional lymph nodes. These results suggest that XL-33-1 has great potential to become a molecular imaging agent for early detection of lymph node tissue with colon cancer metastasis. More importantly, this study clearly demonstrates that DNA ligands selectively recognizing metastatic cancer cells can be readily generated by metastatic-cell-based SELEX for potential applications in metastatic cancer diagnosis and treatment.

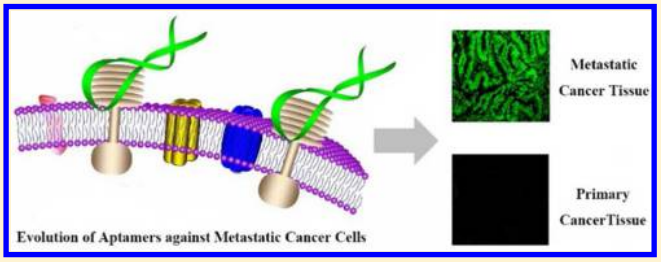

Metastasis, the capability of tumor cells to spread and grow at distant sites, is the primary factor in cancer mortality.[1] For example, more than 20% of patients present with metastatic colon cancer at the time of diagnosis. Even after radical resection, nearly half of colon cancers patients are eventually diagnosed with distant metastases.[2] The main step in tumor progression to metastasis is entry of tumor cells into the circulatory system by penetrating the thin-walled tumor vasculature, including venules, capillaries, and lymphatic channels.[3] Metastasis, especially in sentinel lymph nodes, indicates the original spread of tumors from a primary site.[4] Therefore, as a transport system for tumor cells, examination of regional lymph nodes is a critical part of cancer staging and affects a patient's prognosis and treatment.[5] Traditionally, needle biopsies on enlarged lymph nodes have been examined microscopically to decide whether the lymph node is involved with cancer. This method is highly dependent on the morphologic criteria and the experience of a pathologist.[6] Molecular imaging, however, can give objective and correct assessment of the regional lymph nodes by detecting the abnormal molecules associated with a tumor.[7,8]

In order to specifically target the tissue of interest, several key types of molecular imaging agents have been developed.[9] Owing to the small size, small molecules can cross the vasculature with relative ease, leading to favorable biodistribution. Unfortunately, it requires a time-consuming process to discover, synthesize, and evaluate such small molecular agents.[9] Peptides have some important advantages over small molecules, such as better selectivity and more flexibility in chemical modifications.[10−12] However, peptides have short plasma half-lives because of their susceptibility to proteolytic degradation.[13,14]

Received: February 15, 2015
Accepted: April 13, 2015
Published: April 13, 2015

ACS Publications © 2015 American Chemical Society

DOI: 10.1021/acs.analchem.5b00637
Anal. Chem. 2015, 87, 4941−4948

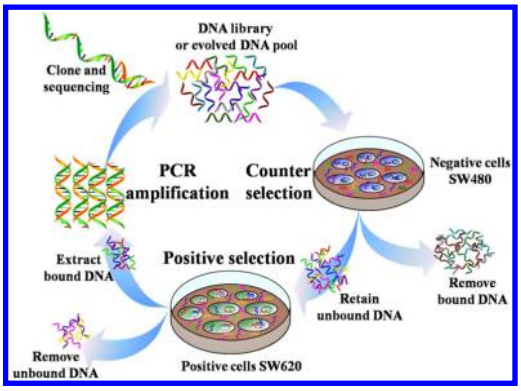

Figure 1. SELEX process for metastatic colon cancer cell SW620. The ssDNA library was incubated with SW480 cells for counter selection. The unbound DNA was eluted and incubated with SW620 cells for positive selection. The SW620-specific DNA was eluted and amplified by PCR for next-round selection or for DNA cloning and sequencing to identify the aptamer candidates.

Unlike small molecules and peptides, monoclonal antibodies (mAbs) can be relatively facile to generate and can bind targets with very high affinity and specificity, thus playing an enormous role as molecular imaging agents.[15] So far, there have over eight radiolabeled mAbs approved as molecular imaging agents by the FDA.[16,17] However, because of their inevitably long residence in the body and their restricted ability to penetrate biological barriers, more effort is needed to improve mAbs.[18]

Nanoparticle-based imaging agents can generate enhanced signal in molecular imaging because of their relatively large size and high surface-area-to-volume ratio.[19] However, these advantages come at the expense of specificity, because of the rapid accumulation of nanoparticles in the liver, spleen, etc.[9]

Aptamers, single-stranded oligonucleotide molecules evolved by systematic evolution of ligands by exponential enrichment (SELEX),[20−23] have become attractive alternatives as molecular imaging agents.[24−29] Apart from their excellent specificity, high affinity, stability, and long shelf-life, advantages of aptamers also include simple synthesis and modification, relatively low molecular weight, and low immunogenesis.[23,30−34]

Using colon cancer as a model, we have used cell-SELEX[22,23] to identify a panel of DNA aptamers which bind to SW620 cells derived from a metastatic site lymph node, using SW480 cells from a primary colon adenocarcinoma of the same patient as negative control. The selected aptamer XL-33 with the best binding affinity and its truncated sequence XL-33-1 with 45 nt were further investigated for specificity, determination of target type, and effect of temperature on their recognition of target cells. Furthermore, laser confocal fluorescence microscopy was used to evaluate the recognition capability of XL-33-1 to colon cancer tissue with metastasis in regional lymph nodes.

EXPERIMENTAL SECTION

Cell Lines and Cell Culture. Human colon cancer cells SW620, SW480, kidney cell HEK-293T, liver cancer cell SMMC-7721, Burkitt's lymphoma B lymphocyte Ramos, lung cancer cell A549, and glioma cells T98G, U251 were obtained from the American Type Culture Collection (ATCC). All cell lines were cultured at 37 °C in a humid atmosphere with 5% CO_2. Cell types SW620, SMMC-7721, Ramos, and A549 were cultured in RPMI-1640 supplemented with 10% fetal bovine serum (FBS) and 0.5 mg/mL penicillin−streptomycin. Cell types SW480, HEK-293T, U251, and T98G were cultured in Dulbecco's modified Eagle's medium (DMEM) supplemented with 10% FBS and 100 U/mL penicillin−streptomycin.

SELEX Library and Primers. The initial library used in this work came from the reference by Tan's group.[35] The library had a randomized region of 45 nucleotides (N_{45}) flanked by two constant regions on both sides for primer annealing and polymerase chain reaction (PCR) amplification (5′-AAG GAG CAG CGT GGA GGA TA-N_{45}-TTA GGG TGT GTC GTC GTG GT-3′). For PCR amplification, forward primer, 5′-FAM-AAG GAG CAG CGT GGA GGA TA-3′, and reverse primer, 5′-biotin-ACC ACG ACG ACA CAC CCT AA-3′, were used. All of the oligonucleotides were synthesized by Shanghai Sangon Biotech Co., Ltd. China.

SELEX Procedures. Colon cancer cell SW620 was used as the target cell line. The initial DNA library (5 nmol) was dissolved thoroughly in 500 μL of binding buffer (4.5 g/L glucose, 5 mM $MgCl_2$, 0.1 mg/mL yeast tRNA, and 1 mg/mL BSA in PBS, pH 7.4). The library was denatured by heating at 95 °C for 5 min and immediately cooled on ice for 10 min. An amount of 5×10^6 SW620 cells was incubated with the initial ssDNA library for 60 min on ice. After incubation, cells were washed with 3 mL of washing buffer (4.5 g/L glucose, 5 mM $MgCl_2$ in PBS, pH 7.4) for 1 min. Cells were harvested from the culture dish using a cell scraper and transferred to 500 μL of water. The bound DNA sequences were eluted by heating at 95 °C for 5 min. The eluted sequences were amplified by PCR with fluorescein isothiocyanate (FITC)- and biotin-labeled primers (5−15 cycles of 30 s at 94 °C, 30 s at 60 °C, and 30 s

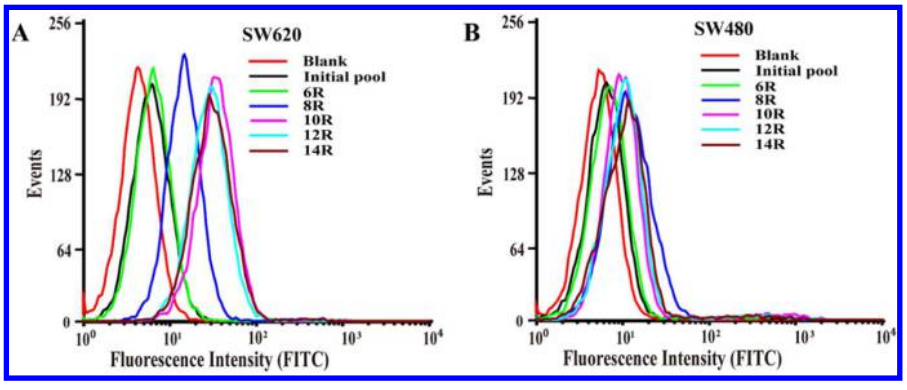

Figure 2. Binding assay of enriched pool with different cells. For the target cell SW620, the fluorescence intensity steadily increased as the selection progressed and reached its maximum level at the 10th round (A), while there was little increase in fluorescence intensity for negative cell SW480 (B). The final concentration of the enriched pool was 250 nM.

DOI: 10.1021/acs.analchem.5b00637
Anal. Chem. 2015, 87, 4941−4948

Table 1. Sequences and Equilibrium Dissociation Constant (K_d) of Selected Aptamers

name	sequence	abundance of sequence (%)	contents of GC (%)	K_d's (nM)
XL-80	**AAGGAGCAGCGTGGAGGATA**GCTGCGACGTTTTTCTCTTTTTTCCT-TAGTTTTAGTTCTATTTAAG**TTTAGGGTGTGTCGTCGTGGT**	27	42.5	14 ± 2
XL-53	**AAGGAGCAGCGTGGAGGATA**TCGGTGTTTATGGTGTCTGTCTTCCT-CATTCATTCGAGCCTTTTG**TTAGGGTGTGTCGTCGTGGT**	3.5	49.4	7 ± 2
XL-33	**AAGGAGCAGCGTGGAGGATA**CCCATCAATGTTACGACCCGC-TAGGGCTGCTGTGCCATCGGGTAA**TTAGGGTGTGTCGTCGTGGT**	2.6	56.5	0.7 ± 0.2
XL-14	**AAGGAGCAGCGTGGAGGATA**CTCACACTCATTACTTTAGCGGGTTC-TAGTGGCCAGGCGCCAGAA**TTAGGGTGTGTCGTCGTGGT**	3.5	54.1	24 ± 7

at 72 °C), followed by 5 min at 72 °C. The PCR product was incubated with streptavidin-coated Sepharose beads (GE Healthcare) for 30 min, followed by alkaline denaturation (with NaOH, 50 mM) and acid neutralization. The surviving ssDNA was desalted and resuspended in binding buffer for the next round of selection.

Prior to the 10th round, the ssDNA pool was incubated only with positive cell SW620 (the number of cells was gradually decreased from 5×10^6 to 2×10^6) on ice. After the 10th round, the library was first incubated with the negative cell SW480 (the number of cells was gradually increase from 2×10^6 to 10^7) to remove nonspecific sequences. The unbound DNA was eluted and then incubated with target cell SW620 for positive selection. To acquire more specific and high-affinity aptamers, the positive incubation time was decreased from 60 to 30 min and the washing time was increased gradually from 30 s to 6 min as the number of selection rounds increased. Meanwhile, the negative incubation time was gradually increased from 30 to 60 min, and the concentration of DNA used in the negative selection was gradually decreased from 360 to 200 pmol.

Flow Cytometric Analysis of Enrichment Pools. To monitor the enrichment, 250 nM FAM-labeled ssDNA pools were incubated with 2×10^5 target or negative cells on ice for 30 min. Cells were washed with 500 μL of washing buffer for three times and then resuspended in 1000 μL of washing buffer. The fluorescence signal was measured by a FACScan cytometer in triplicate (Becton Dickinson Immunocytometry Systems) by counting 10 000 events. The initial library was used as a negative control.

Cloning and DNA Sequencing of Enriched Pools. When the fluorescence intensity of the selected pools was noticeably greater than that of the initial pool, the enrichment process was completed. The resulting pool from the 14th round was PCR amplified, cloned, and sequenced (Shanghai Sangon). Using ClustalX2.0.3 software, the resulting 114 sequences were subjected to multiple sequence alignment analysis.[36] On the basis of the abundance in the cloned sequences and the contents of GC (Supporting Information Table S1), four representative sequences from selected pools were chosen and then chemically synthesized (Shanghai Sangon) for further study.

Selectivity of Aptamers. To evaluate the selectivity of the aptamers, target cell line SW620, negative cell line SW480, and other human cell lines (kidney cell HEK-293T, liver cancer cell SMMC-7721, Burkitt's lymphoma B lymphocyte Ramos, lung cancer cell A549, and glioma cells T98G, U251) were incubated with the chosen aptamers and studied using flow cytometry.

Binding Analyses. SW620 cells (1×10^5) were incubated with a series of concentrations of FAM-labeled aptamer in 200 μL of binding buffer on ice for 30 min. After three times of washing with 500 μL of washing buffer, cells were resuspended in 1000 μL of binding buffer and analyzed by flow cytometry. The FAM-labeled initial pool was used as a negative control. All of the binding assays were repeated three times. The dissociation constants (K_d) were acquired by fitting the dependence of fluorescence intensity on the aptamer concentration, according to the equation $Y = B_{max}X/(K_d + X)$ by SigmaPlot software (Jandel Scientific).

Proteinase Treatment. Target cell SW620 (1×10^5) was washed with 1 mL of PBS and then incubated with 200 μL of 0.05% trypsin/0.53 nM EDTA or 0.02 μg/mL proteinase K in PBS buffer at 37 °C for 2 min, respectively. After adding FBS to inhibit proteinase and washing with 2 mL of washing buffer, cells were used in the binding assay as described above.

Effect of Temperature on Binding. Aptamers generated on ice can be used for more assay platforms if they can bind to the target at physiological temperature. Therefore, the binding assays of aptamers were also performed at 37 °C with a 30 min incubation.

Imaging of Tissue Sections. The tissue microarray was obtained from US Biomax (Xi'an AiLiNa Biotechnology Co., Ltd. China). Tissue pretreatment was performed as described in the literature.[37,38] Briefly, tissue sections were deparaffinized in xylene (5 min × 3), then rehydrated through an ethanol dilution series: 100%, 95%, 80%, and 70% for 5, 5, 3, and 3 min, respectively. After washing with PBS buffer (pH 8.0), the hydrated tissue sections were heated in citrate buffer (0.01 M, pH 6.0) at 95 °C for 2 min to retrieve antigens. The prepared tissue sections were blocked with 0.05% tRNA for 60 min and then incubated with 250 nM FAM-labeled XL-33-1 in 200 μL of binding buffer for 30 min on ice in dark. A Leica TCS SP5 microscope (Leica Microsystems CMS GmbH, Germany) was applied for imaging. FAM was excited by a 488 nm argon ion laser.

RESULTS AND DISCUSSION

Enrichment of Aptamers Specific for Metastatic Colon Cancer Cells. For generating aptamers specifically against metastatic colon cancer, a pair of very similar cell lines was adopted in our study. According to the information provided by ATCC, cell line SW480 was established from a primary adenocarcinoma of the colon. The SW620 cell line was isolated from the same patient's tumor, but it was derived from a lymph node metastasis. With cell line SW620 as the target and SW480 as the control, cell-SELEX (Figure 1) was used for the enrichment of aptamers. Because the target and the control were similar to a great extent, no control cells were used in the SELEX process prior to the 10th round to avoid failure of the enrichment process. The library was incubated with target cell SW620. After washing, the bound DNA was eluted and amplified by PCR as the library for next-round selection. After the 10th round of selection, the library was first incubated with the negative cell SW480 to remove nonspecific sequences. The unbound DNA was eluted and then incubated with target cell SW620 for positive selection. After the last round of selection, the enriched DNA pool was cloned and sequenced for identifying the individual sequence information.

The enrichment of DNA library was monitored by flow cytometry. As Figure 2A shows, the fluorescence intensity of the

DOI: 10.1021/acs.analchem.5b00637
Anal. Chem. 2015, 87, 4941−4948

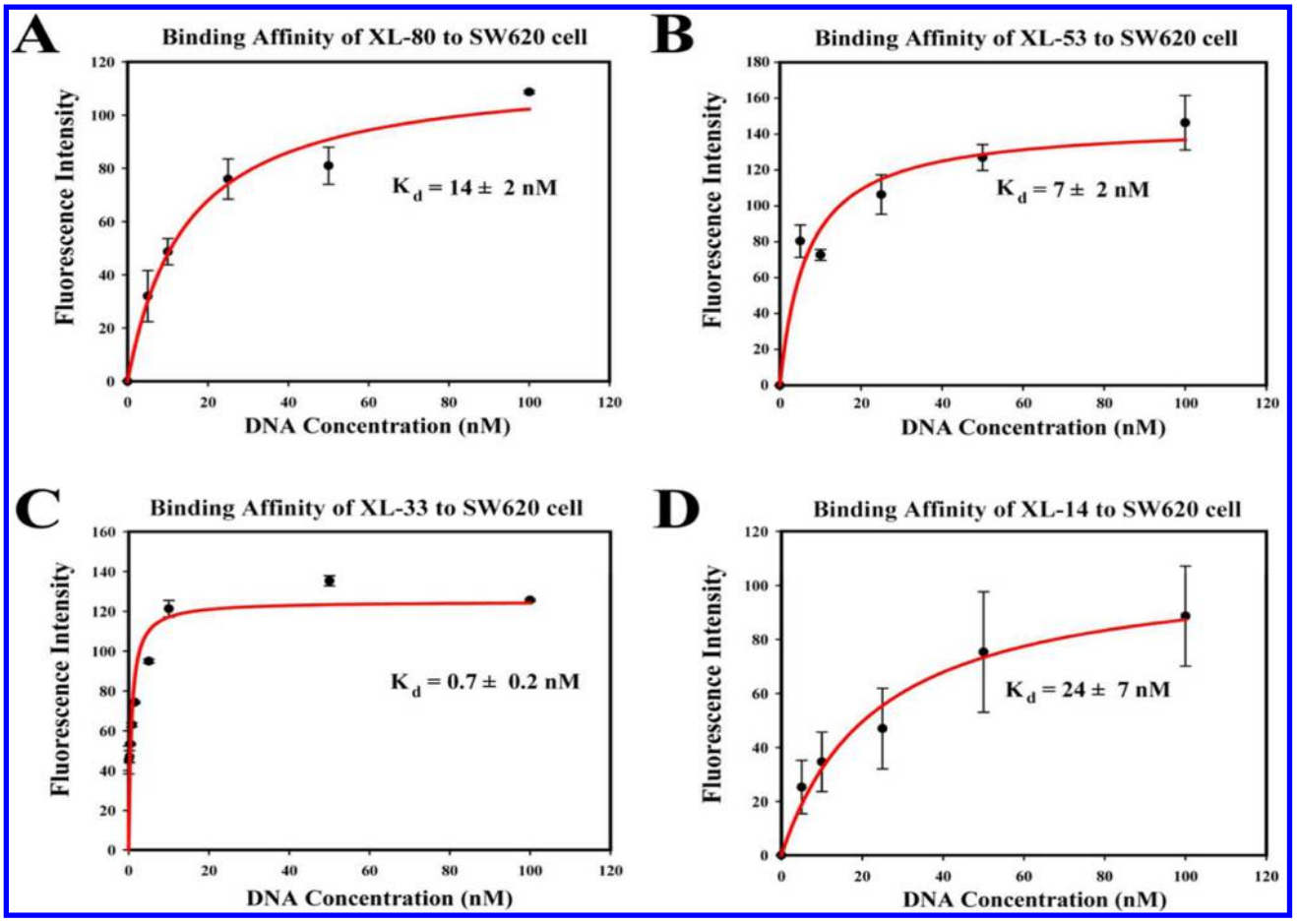

Figure 3. Equilibrium dissociation constant (K_d) of selected aptamer XL-80 (A), XL-53 (B), XL-33 (C), and XL-14 (D) for SW620.

Table 2. Truncated Sequences from Selected Aptamer Candidates

name	sequence
XL-80-1	GCTGCGACGTTTTTCTCTTTTTTCCTTAGTTTTAGTTCTATTTAAGT
XL-53-1	TCGGTGTTTATGGTGTCTGTCTTCCTCATTCATTCGAGCCTTTTG
XL-33-1	CCCATCAATGTTACGACCCGCTAGGGCTGCTGTGCCATCGGGTAA
XL-14-1	CTCACACTCATTACTTTAGCGGGTTCTAGTGGCCAGGCGCCAGAA

target cell-ssDNA complex steadily increased with the increasing of the number of selection rounds prior to the 10th round, and the fluorescence intensity remained approximately constant from the 10th round to the 14th round. In contrast, almost no fluorescence change was observed with the negative cell SW480 (Figure 2B). These results suggested that DNA sequences with specific recognition to target cell SW620 had reached maximum enrichment. The enriched DNA pool of the 14th round was cloned and sequenced.

Binding Affinities of DNA Aptamer Candidates. After sequence analysis using ClustalX2.0.3 software, the sequences were divided into 11 families based on the homologous similarity of sequences. According to the abundance in the cloned sequences and the GC contents, four representative sequences were chosen and synthesized for further characterization. As shown in Table 1, selected sequences XL-80, XL-53, XL-33, and XL-14 accounted for 27%, 3.5%, 2.6%, and 3.5% of all identified sequences, respectively, and the contents of GC in each sequence were 42.5%, 49.4%, 56.5%, and 54.1%, respectively. Using flow cytometry, the binding abilities of four selected sequences to target cell SW620 were assessed. As shown in Figure 3 and Table 1, the K_d values of all four sequences were in a very low nanomolar range, especially XL-33 with 0.7 nM. The results demonstrated the high binding affinity of selected sequences against target cell SW620.

Sequence Optimization of Selected Aptamer Candidates. The modification and synthesis of long sequences are expensive and laborious, seriously suppressing the wide application of aptamers. Therefore, the selected aptamer candidates underwent sequence optimization by removing the unnecessary nucleotides, while maintaining the original affinity. We optimized these sequences by truncating their marginal sequences, mainly the primer sequences. The four truncated sequences XL-80-1, XL-53-1, XL-33-1, and XL-14-1 are shown in Table 2. Subsequent aptamer binding assays showed that only XL-33-1 has similar binding to the target cell SW620 compared to the original XL-33 (Figure 4C). XL-80-1 (Figure 4A), XL-53-1 (Figure 4B), and XL-14-1(Figure 4D) hardly bound to SW620 cells, suggesting that the primer is an essential part of these aptamers for target cell binding. Similar to their parent sequences, none of these truncated sequences bound to the negative cell SW480.

DOI: 10.1021/acs.analchem.5b00637
Anal. Chem. 2015, 87, 4941−4948

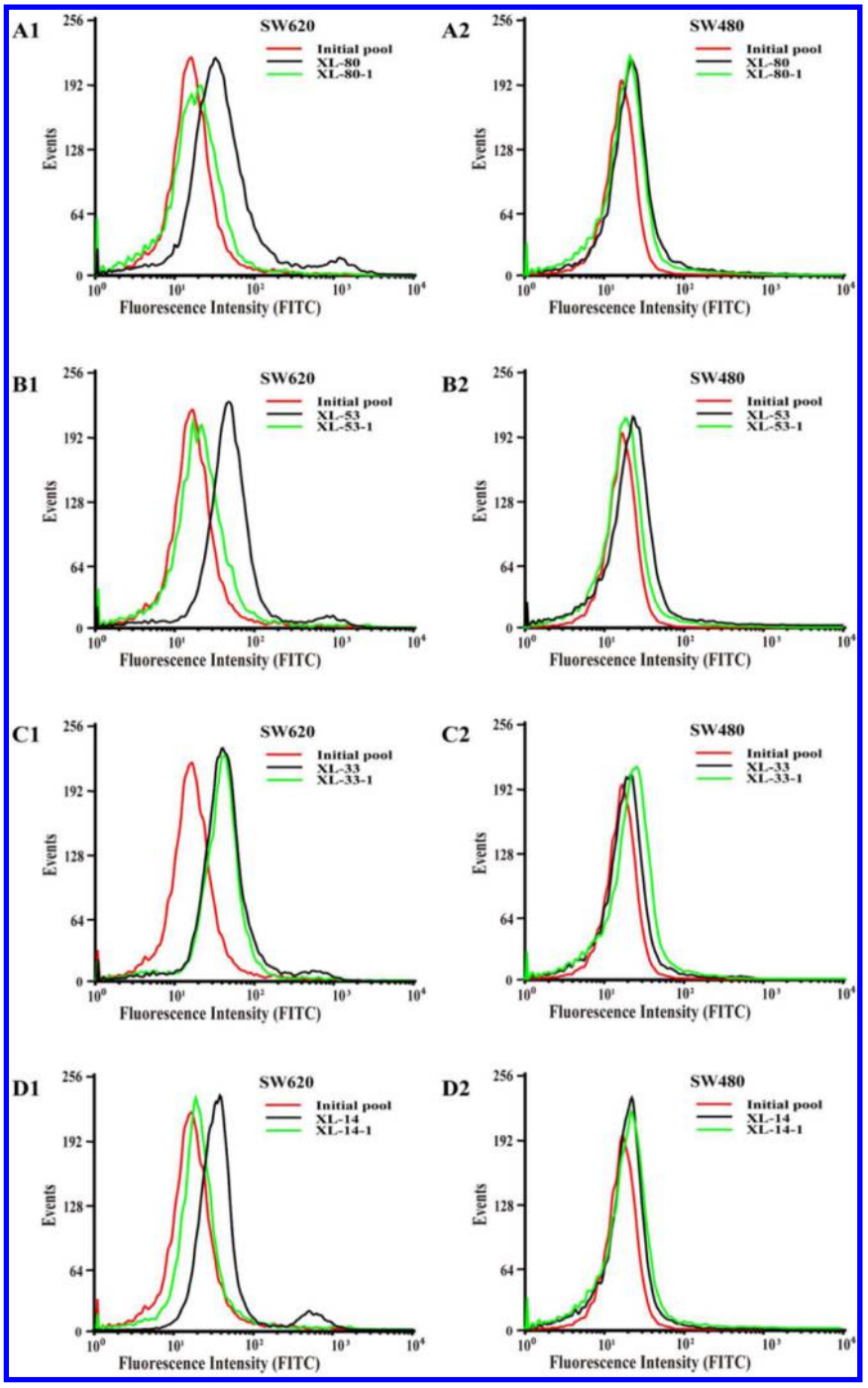

Figure 4. Binding of truncated sequences XL-80-1 with the SW620 (A1) and SW480 (A2), XL-53-1 with the SW620 (B1) and SW480 (B2), XL-33-1 with the SW620 (C1) and SW480 (C2), XL-14-1 with the SW620 (D1) and SW480 (D2).

Binding Affinity of Truncated Sequence XL-33-1. The binding ability of truncated sequence XL-33-1 to target cell SW620 was assessed by flow cytometry. As shown in Figure 5, the K_d value of XL-33-1 was 7 nM. Results of the binding assays mentioned above and K_d values demonstrated that we have obtained a truncated sequence with only 45 nt with similar recognition capability and selectivity as XL-33 (K_d = 0.7 nM).

Specificity of Aptamers. Because of its good recognition ability to the target cells, the truncated sequence XL-33-1 was further characterized. In order to demonstrate its specificity, the FAM-labeled truncated sequence XL-33-1 was tested with colon cancer cell SW620 from the metastatic site lymph node, SW480 from the primary adenocarcinoma of the colon and cells of other body systems, including kidney cell HEK-293T, liver cancer cell SMMC-7721, Burkitt's lymphoma B lymphocyte Ramos, lung cancer cell A549, and glioma cells T98G, U251.

Target cell SW620 incubated with truncated sequence XL-33-1 exhibited remarkably higher fluorescence intensity than that of initial library (Figure 6A), while the negative cell SW480 (Figure 6B) and other human cell types [HEK-293T (Figure 6C), SMMC-7721 (Figure 6D), Ramos (Figure 6E), A549 (Figure 6F), T98G (Figure 6G), and U251 (Figure 6H)] incubated with truncated sequence XL-33-1 had almost no change in fluorescence intensity compared with that of the initial library. These results

DOI: 10.1021/acs.analchem.5b00637
Anal. Chem. 2015, 87, 4941−4948

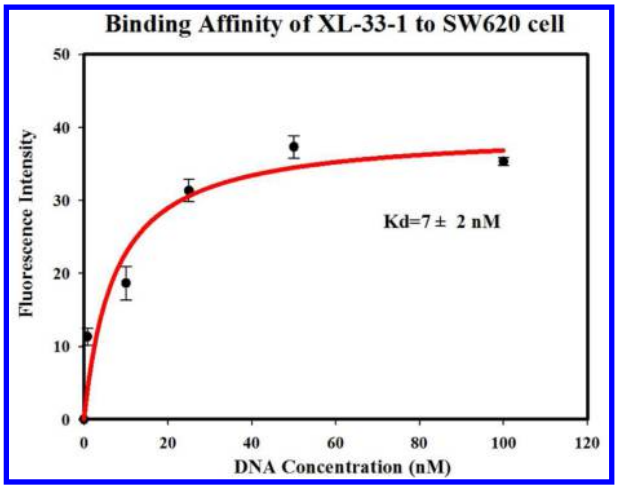

Figure 5. Equilibrium dissociation constant (K_d) of truncated sequence XL-33-1 for SW620.

indicated that the truncated sequence XL-33-1 derived from the metastatic site lymph node is capable not only of identifying target SW620 cells from different body systems, but also of distinguishing the subtle difference of the cell of primary adenocarcinoma of the colon from the same patient. The above results demonstrated that the truncated sequence XL-33-1 can selectively recognize targets presenting on the surface of SW620 cells and further suggested that their recognition targets are probably exclusive on metastatic cell line SW620.

Determination of Target Type. In order to investigate whether the aptamer target is a protein on the cell membrane, FAM-labeled truncated sequence XL-33-1 was incubated with trypsin- or proteinase K-treated cells and then analyzed using flow cytometry. As shown in Figure 7, after treatment with trypsin for 2 min, the truncated sequence XL-33-1 lost its binding affinity considerably compared with no treatment. After treatment with proteinase K for 2 min, the truncated sequence XL-33-1 showed only slightly decreased binding affinity compared with no treatment. The change in binding efficiency after trypsin treatment suggested that the target of truncated sequence XL-33-1 may be a protein or closely related to proteins.

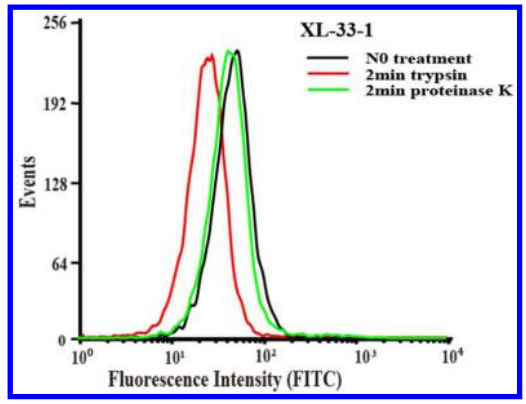

Figure 7. Binding of truncated sequence XL-33-1 to trypsin- or proteinase-treated SW620 cells. The final concentration of FAM-labeled sequence was 250 nM.

Temperature Effect on Aptamer Binding Ability. At physiological temperature, DNA can be nonspecifically uptaken by cells through endocytosis. This will cause the loss of important sequences, delay of enrichment, or even the failure of selection. However, it will greatly increase the flexibility of an aptamer's application if it can identify the target under physiological conditions. We therefore tested the binding of the truncated sequence XL-33-1 at 37 °C. As shown in Figure 8, the signal strengths of SW620 cells incubated with XL-33-1 (Figure 8A) significantly shifted compared with that of initial pool at 37 °C. On the other hand, the fluorescence intensity of SW480 cells incubated with XL-33-1 (Figure 8B) showed almost no change compared with initial pool at 37 °C. Binding affinity of XL-33-1 against SW620 at 37 °C was found to be 322 nM. These results demonstrated the applicability of XL-33-1 at physiological temperature and provided an important foundation for the future study of aptamer-based assays, such as diagnostics, biomarker discovery, and targeted therapy.

Imaging of Metastatic Colon Cancer Tissues. Since the target cell SW620 was derived from lymph node metastasis, we speculated whether the XL-33-1 can specifically recognize metastatic colon cancer tissue or lymph node tissue with colon cancer metastasis. Laser confocal fluorescence microscopy was

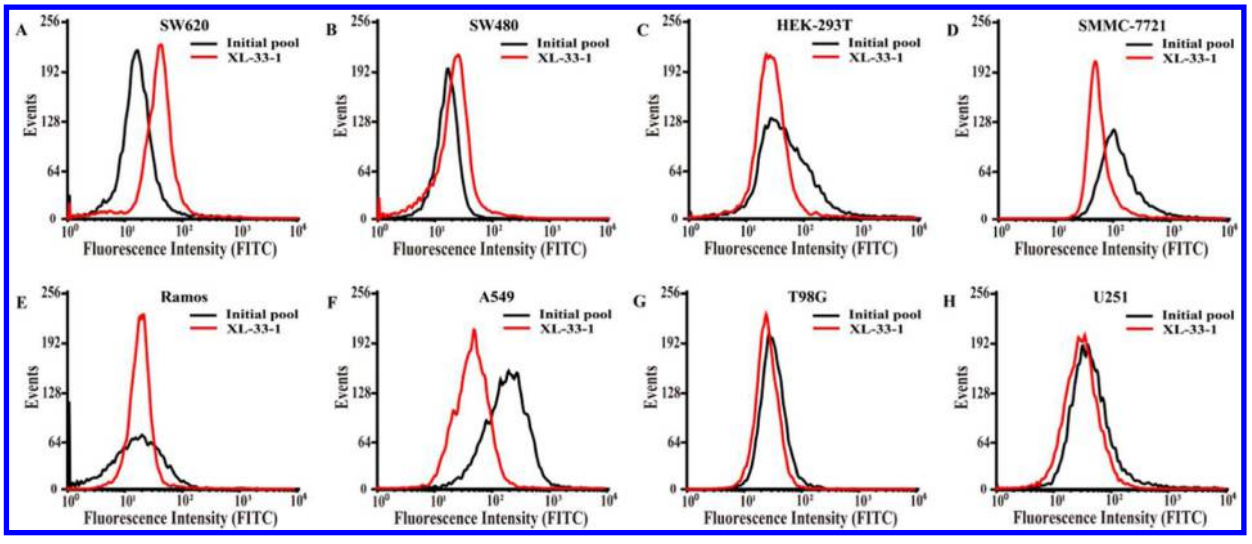

Figure 6. Binding of truncated sequences XL-33-1 with SW620 cells (A), SW480 cells (B), HEK-293T cells (C), SMMC-7721 cells (D), Ramos cells (E), A549 cells (F), T98G cells (G), and U251 cells (H). The concentration of sequences was 250 nM.

DOI: 10.1021/acs.analchem.5b00637
Anal. Chem. 2015, 87, 4941−4948

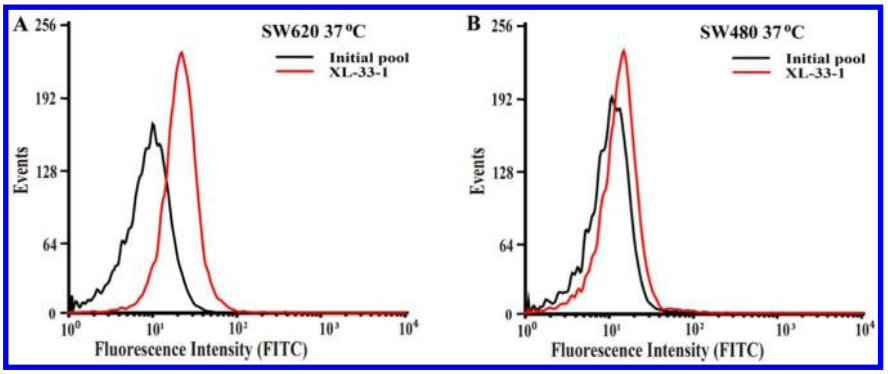

Figure 8. Flow cytometry assay for the binding capacity of XL-33-1 to SW620 (A) or SW480 (B) at 37 °C.

applied for imaging metastatic colon cancer tissues with FAM-labeled XL-33-1 to acquire visible images and statistical data (Figure 9 and Table 3). Obviously, the colon cancer tissue with metastasis in regional lymph nodes (Figure 9A1−A4) and lymph node tissue with colon cancer metastasis (Figure 9C1−C4) gave bright green fluorescence after incubating with FAM-labeled XL-33-1. Colon cancer tissue with no regional lymph node metastasis (Figure 9B1−B4), liver tissue with colon cancer metastasis (Figure 9D1−D4), normal colon tissue (Figure 9E1−E4), and FAM-labeled random sequences incubated with colon cancer tissue with metastasis in regional lymph node (Figure 9, parts F1 and F2) and lymph node tissue with colon cancer metastasis (Figure 9, parts F3 and F4) exhibited negligible fluorescence signal.

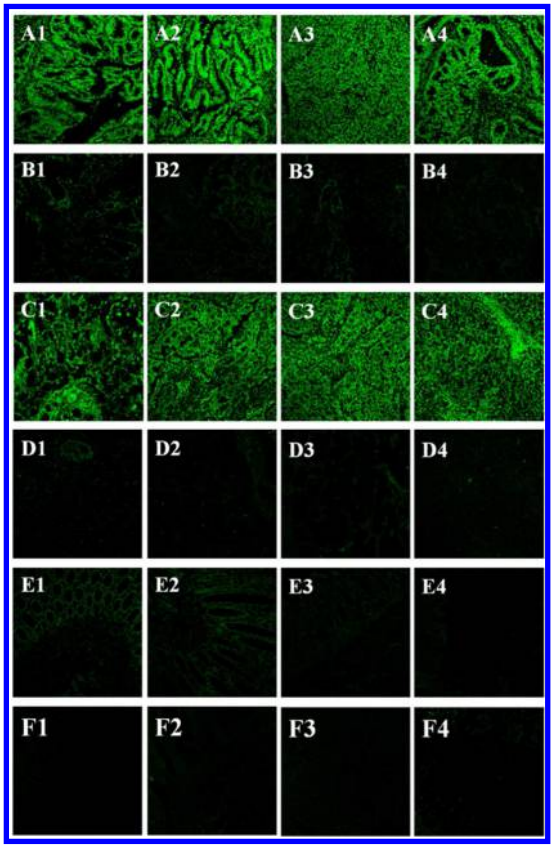

Figure 9. Fluorescence images of colon cancer tissue with metastasis in regional lymph node (A1−A4), colon cancer tissue with no regional lymph node metastasis (B1−B4), lymph node tissue with colon cancer metastasis (C1−C4), liver tissue with colon cancer metastasis with XL-33-1 (D1−D4), and normal colon tissue (E1−E4) using FAM labeled XL-33-1. Fluorescence images of colon cancer tissue with metastasis in regional lymph node (F1 and F2) and lymph node tissue with colon cancer metastasis using FAM labeled random sequences (F3 and F4).The final concentration of FAM-labeled DNA was 250 nM.

Table 3. Statistical Data from Confocal Images of Tissue Sections Stained with XL-33-1

tissue section	no. of tissues	positive rate (%)
colon cancer tissue with metastasis in regional lymph node	71	81.7
colon cancer tissue with no regional lymph node metastasis	18	33.3
lymph node tissue with colon cancer metastasis	58	72.4
liver tissue with colon cancer metastasis	5	20.0
normal colon tissue	11	18.2

The percentages of positive ratings for each tissue type in Table 3 clearly showed that XL-33-1 is highly specific to the metastatic tumor tissue (81.7%) and to lymph node tissue with cancer metastasis (72.4%) compared to the other tissues tested (all less than 35%). These results clearly illustrated that XL-33-1 generated from cell-SELEX can specifically recognize the corresponding metastatic tumor tissues or lymph node tissue with corresponding cancer metastasis. Therefore, the XL-33-1 can be potentially applied as an effective molecular diagnostic reagent for recognition of metastatic colon tumor tissue, which is of great significance for colon cancer diagnosis and treatment.

CONCLUSIONS

In summary, we have successfully generated a panel of aptamers that specifically recognize colon cancer cell SW620 using cell-SELEX after 14 rounds of selection. The K_d values of these selected aptamers are in the low-nanomolar range, with XL-33 having the lowest K_d (0.7 nM). Structural studies generated a truncated sequence XL-33-1 with only 45 nt with the same recognition capability as XL-33 against target cell SW620. The truncated sequence XL-33-1 can identify subtle differences from the cells of primary adenocarcinoma of the colon from the same patient. The target of XL-33-1 has been preliminarily determined as a membrane protein on the cell surface. At physiological temperature, XL-33-1 also has the specific recognition capability to SW620. Tissue imaging results showed that XL-33-1 displayed an 81.7% detection rate against colon cancer tissue with metastasis in regional lymph nodes, 72.4% positive rate against lymph node tissue with colon cancer metastasis. These results suggest that XL-33-1 holds great potential to become a molecular imaging probe for early detection of cancer metastasis. More

DOI: 10.1021/acs.analchem.5b00637
Anal. Chem. 2015, 87, 4941−4948

importantly, this study clearly demonstrates that DNA ligands selectively recognizing metastatic cancer cells can be readily generated by metastatic-cell-based SELEX for potential applications in metastatic cancer diagnosis and treatment.

■ ASSOCIATED CONTENT

Supporting Information

Table S1 (DNA sequencing results). This material is available free of charge via the Internet at http://pubs.acs.org.

■ AUTHOR INFORMATION

Corresponding Author

*Phone: +86 592-218-7601. Fax: +86 592-218-9959. E-mail: cyyang@xmu.edu.cn.

Notes

The authors declare no competing financial interest.

■ ACKNOWLEDGMENTS

We thank the National Science Foundation for Distinguished Young Scholars of China (21325522), the National Science Foundation of China (91313302, 21205100, 21275122, 21422506, 21435004), the Natural Science Foundation of Fujian Province (2013J01061), and the National Basic Research Program of China (2013CB933703) for financial support.

■ REFERENCES

(1) Zueva, E.; Rubio, L. I.; Ducongé, F.; Tavitian, B. *Int. J. Cancer* **2011**, *128*, 797−804.
(2) Simmonds, P. C.; Primrose, J. N.; Colquitt, J. L.; Garden, O. J.; Poston, G. J.; Rees, M. *Br. J. Cancer* **2006**, *94*, 982−999.
(3) Fidler, I. J. *Nat. Rev. Cancer* **2003**, *3*, 453−458.
(4) Hirakawa, S. *Cancer Sci.* **2009**, *100*, 983−989.
(5) Das, S.; Skobe, M. *Ann. N. Y. Acad. Sci.* **2008**, *021*, 235−241.
(6) Sobin, L. H.; Fleming, I. D. *Cancer* **1997**, *80*, 1803−1804.
(7) Weissleder, R. *Science* **2006**, *312*, 1168−1171.
(8) Blasberg, R. G. *Mol. Cancer Ther.* **2003**, *2*, 335−343.
(9) James, M. L.; Gambhir, S. S. *Physiol. Rev.* **2012**, *92*, 897−965.
(10) Hausner, S. H.; Marik, J.; Gagnon, M. K.; Sutcliffe, J. L. *J. Med. Chem.* **2008**, *51*, 5901−5904.
(11) Schottelius, M.; Wester, H. J. *Methods* **2009**, *48*, 161−177.
(12) Sato, A. K.; Viswanathan, M.; Kent, R. B.; Wood, C. R. *Curr. Opin. Biotechnol.* **2006**, *17*, 638−642.
(13) Mading, P.; Fuchtner, F.; Wust, F. *Appl. Radiat. Isot.* **2005**, *63*, 329−332.
(14) Marik, J.; Sutcliffe, J. L. *Appl. Radiat. Isot.* **2007**, *65*, 199−203.
(15) Wallis de Vries, B. M.; van Dam, G. M.; Tio, R. A.; Hillebrands, J. L.; Slart, R. H.; Zeebregts, C. J. *J. Vasc. Surg.* **2008**, *48*, 1620−1629.
(16) van Dongen, G. A.; Visser, G. W.; Lub-de Hooge, M. N.; de Vries, E. G.; Perk, L. R. *Oncologist* **2007**, *12*, 1379−1389.
(17) Olafsen, T.; Wu, A. M. *Semin. Nucl. Med.* **2010**, *40*, 167−181.
(18) Kobayashi, H.; Choyke, P. L. *Acc. Chem. Res.* **2011**, *44*, 83−90.
(19) Jokerst, J. V.; Lobovkina, T.; Zare, R. N.; Gambhir, S. S. *Nanomedicine* **2011**, *6*, 715−728.
(20) Ellington, A. D.; Szostak, J. W. *Nature* **1990**, *346*, 818−822.
(21) Tuerk, C.; Gold, L. *Science* **1990**, *249*, 505−510.
(22) Shangguan, D.; Li, Y.; Tang, Z.; Cao, Z. C.; Chen, H. W.; Mallikaratchy, P.; Sefah, K.; Yang, C. J.; Tan, W. *Proc. Natl. Acad. Sci. U. S. A.* **2006**, *103*, 11838−11843.
(23) Sefah, K.; Shangguan, D.; Xiong, X.; O'Donoghue, M. B.; Tan, W. *Nat. Protoc.* **2010**, *5*, 1169−1185.
(24) Wang, A. Z.; Farokhzad, O. C. *J. Nucl. Med.* **2014**, *55*, 353−356.
(25) Jayasena, S. D. *Clin. Chem.* **1999**, *45*, 1628−1650.
(26) Hu, J.; Wu, J.; Li, C.; Zhu, L.; Zhang, W. Y.; Kong, G.; Lu, Z.; Yang, C. J. *ChemBioChem* **2011**, *12*, 424−430.
(27) Wu, J.; Wang, C.; Li, X.; Song, Y.; Wang, W.; Li, C.; Hu, J.; Zhu, Z.; Li, J.; Zhang, W.; Lu, Z.; Yang, C. J. *PLoS One* **2012**, *7*, e46393.
(28) Zhang, W. Y.; Zhang, W.; Liu, Z.; Li, C.; Zhu, Z.; Yang, C. J. *Anal. Chem.* **2011**, *84*, 350−355.
(29) Zhu, G.; Zheng, J.; Song, E.; Donovan, M.; Zhang, K.; Liu, C.; Tan, W. *Proc. Natl. Acad. Sci. U. S. A.* **2013**, *110*, 7998−8003.
(30) Osborne, S. E.; Matsumura, I.; Ellington, A. D. *Curr. Opin. Chem. Biol.* **1997**, *1*, 5−9.
(31) Famulok, M.; Hartig, J. S.; Mayer, G. *Chem. Rev.* **2007**, *107*, 3715−3743.
(32) Hu, M.; Zhang, K. *Future Oncol.* **2013**, *9*, 369−376.
(33) Saini, K. S.; Taylor, C.; Ramirez, A.-J.; Palmieri, C.; Gunnarsson, U.; Schmoll, H. J.; Dolci, S. M.; Ghenne, C.; Metzger-Filho, O.; Skrzypski, M.; Paesmans, M.; Ameye, L.; Piccart-Gebhart, M. J.; de Azambuja, E. *Ann. Oncol.* **2012**, *23*, 853−859.
(34) Tan, W.; Donovan, M. J.; Jiang, J. *Chem. Rev.* **2013**, *113*, 2842−2862.
(35) Tang, Z.; Shangguan, D.; Wang, K.; Shi, H.; Sefah, K.; Mallikratchy, P.; Chen, H. W.; Li, Y.; Tan, W. *Anal. Chem.* **2007**, *79*, 4900−4907.
(36) Thompson, J. D.; Gibson, T. J.; Plewniak, F.; Jeanmougin, F.; Higgins, D. G. *Nucleic Acids Res.* **1997**, *25*, 4876−4882.
(37) Zhao, Z.; Xu, L.; Shi, X.; Tan, W.; Fang, X.; Shangguan, D. *Analyst* **2009**, *134*, 1808−1814.
(38) Chen, H. W.; Medley, C. D.; Sefah, K.; Shangguan, D.; Tang, Z.; Meng, L.; Smith, J. E.; Tan, W. *ChemMedChem* **2008**, *3*, 991−1001.

DOI: 10.1021/acs.analchem.5b00637
Anal. Chem. 2015, 87, 4941−4948